

Current Biology, Volume 31

Supplemental Information

**Evolution of crossover interference enables
stable autopolyploidy by ensuring pairwise
partner connections in *Arabidopsis arenosa***

Chris Morgan, Martin A. White, F. Chris H. Franklin, Denise Zickler, Nancy Kleckner, and Kirsten Bomblies

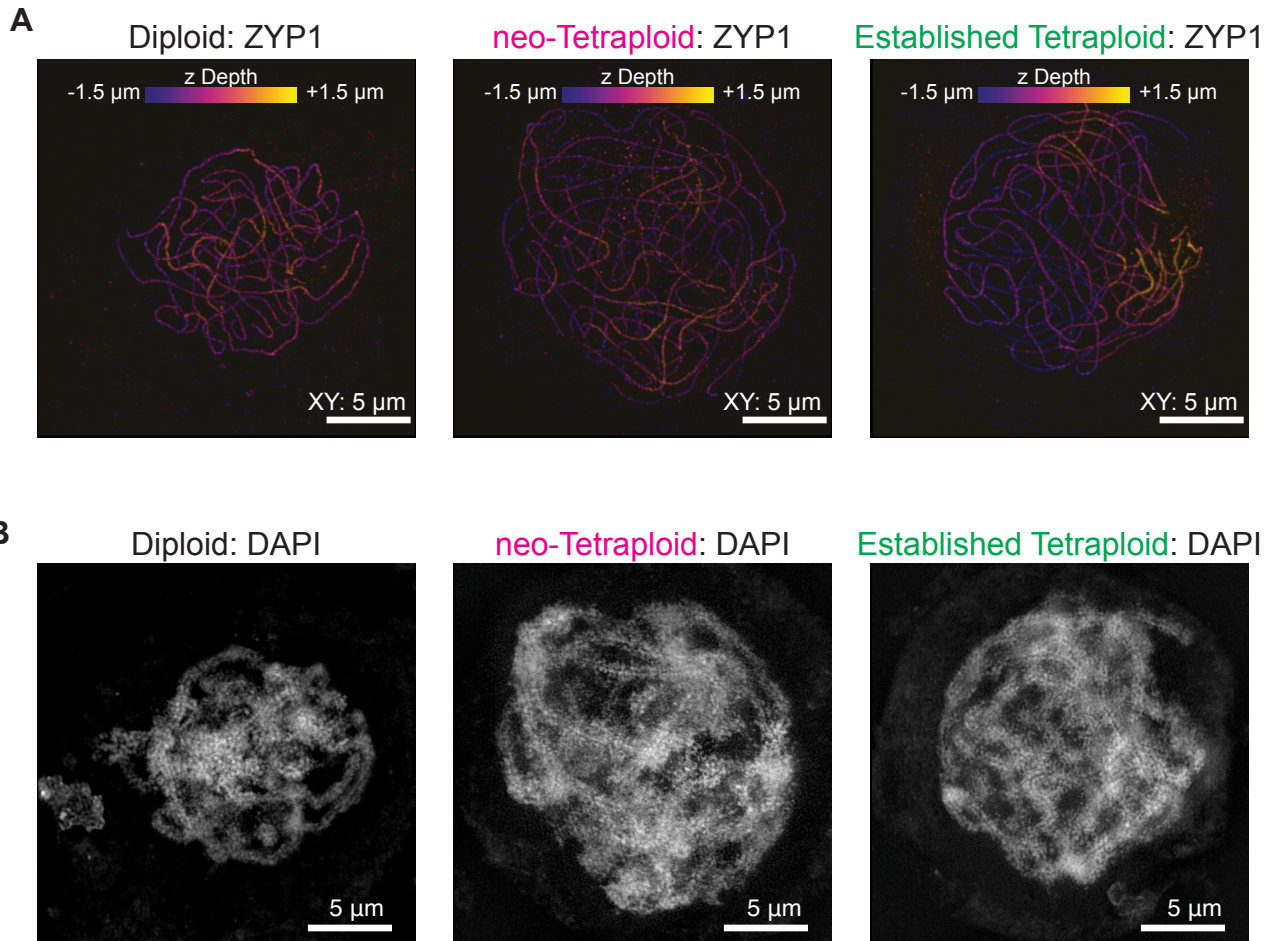


Figure S1. Additional 3D immunofluorescence SIM images of *A. arenosa* diploid, neo-tetraploid and established tetraploid late pachytene nuclei. Related to Figure 2 and Video S1.

A. Mildly squashed pachytene nuclei still retain significant 3D character. Maximum intensity z-projections of ZYP1 images of pachytene diploid, neo-tetraploid and established tetraploid nuclei presented in Figure 2, color coded for z-depth. Scale bars show 5 μm.

B. DAPI images showing the DNA of the pachytene diploid, neo-tetraploid and established tetraploid nuclei presented in Figure 2. Scale bars show 5 μm.

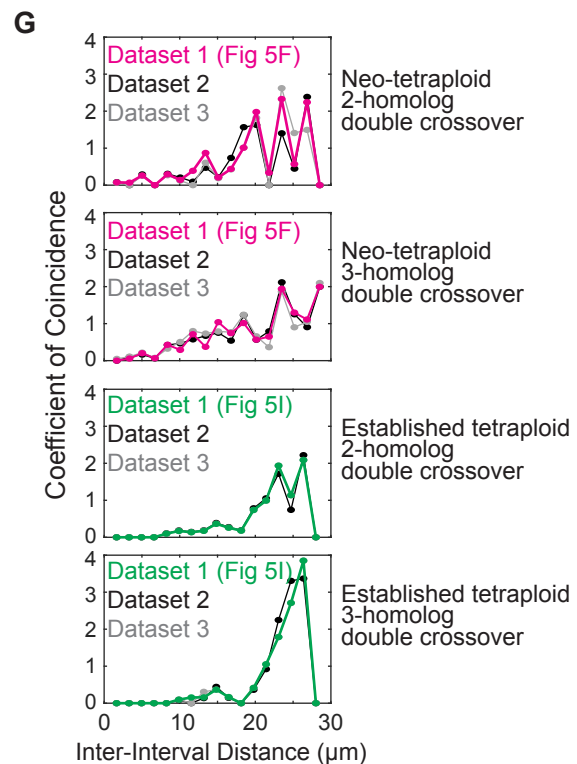
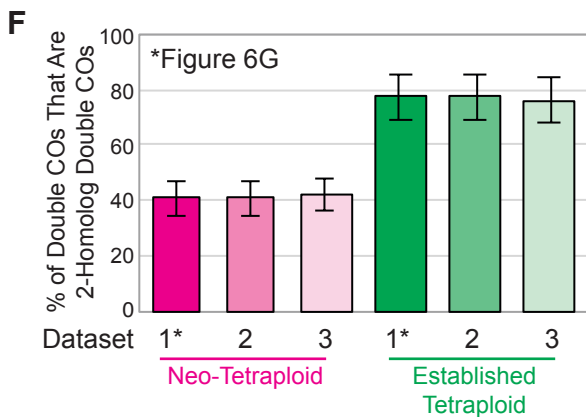
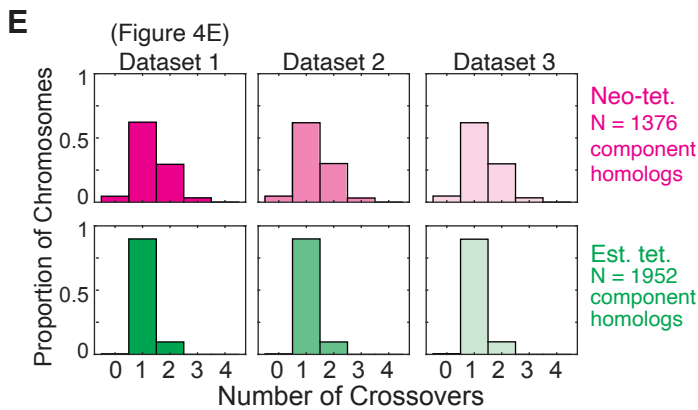
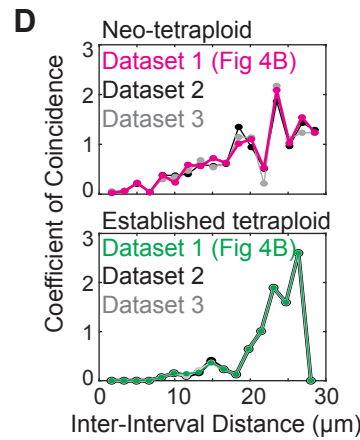
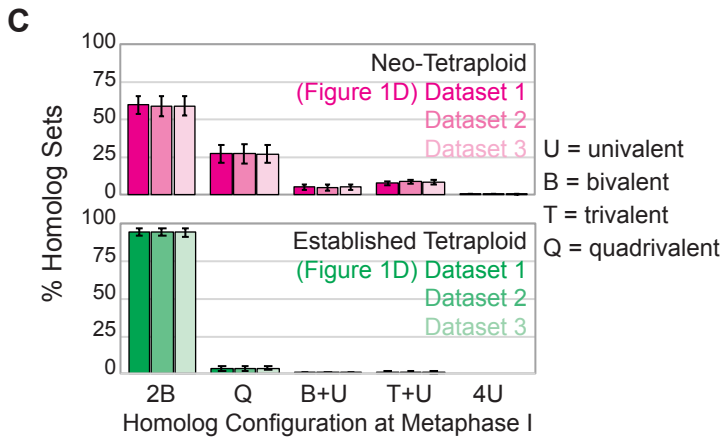
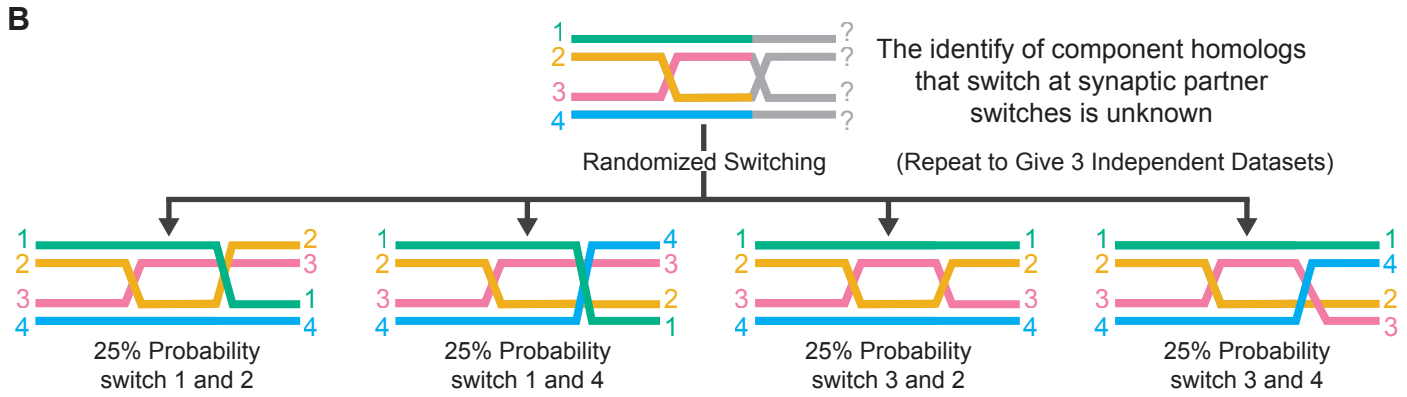
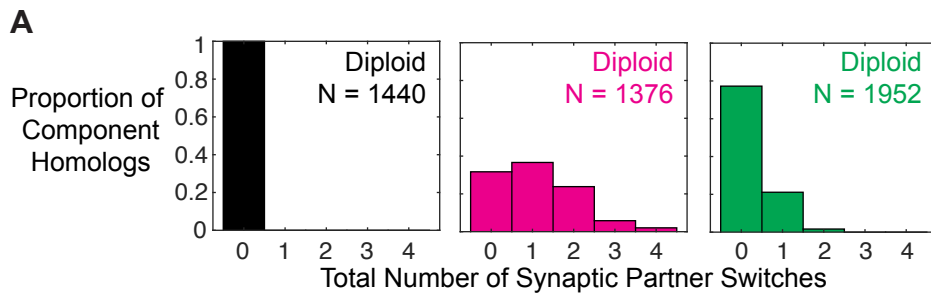


Figure S2. Randomized switching of component homologs at synaptic partner switches. Related to Figure 1, Figure 3, Figure 4, Figure 5 and Figure 6.

A. Distribution of number of synaptic partner switches per component homolog.

B. Component homologs of pachytene quadrivalents with two or more synaptic partner switches cannot be unambiguously defined. For each pachytene quadrivalent, one of each paired component homolog was randomly chosen to switch partners. Three independent component homolog datasets were generated in such a manner for both the neo- and established tetraploid to test the impact of this unknown on measurements.

C. Predicted metaphase I configurations of total homolog sets for each of the three independent component homolog datasets for *A. arenosa* neo-tetraploid and established tetraploid nuclei as defined by component homolog analysis of crossovers along pachytene chromosomes. Error bars show standard error of the mean, N = 4 plants for both neo-tetraploid and established tetraploid.

D. Coefficient of coincidence analysis for each of the three independent component homolog datasets for *A. arenosa* neo-tetraploids and established tetraploids. N = 486 and 622 component homologs between 27 and 33 μm in length for neo-tetraploid and established tetraploid respectively.

E. Distribution of numbers of crossovers per component homolog for each of the three independent component homolog datasets for *A. arenosa* neo-tetraploids and established tetraploids.

F. The percentage of observed double crossovers that are two-homolog double crossovers for each of the three independent component homolog datasets for *A. arenosa* neo-tetraploids and established tetraploids. Error bars show standard error of the mean, N = 4 plants for neo-tetraploid and established tetraploid.

G. Coefficient of coincidence analysis for 2-homolog and 3-homolog double crossovers for each of the three independent component homolog datasets for *A. arenosa* neo-tetraploids and established tetraploids. N = 486 and 622 component homologs between 27 and 33 μm in length for neo-tetraploid and established tetraploid respectively.

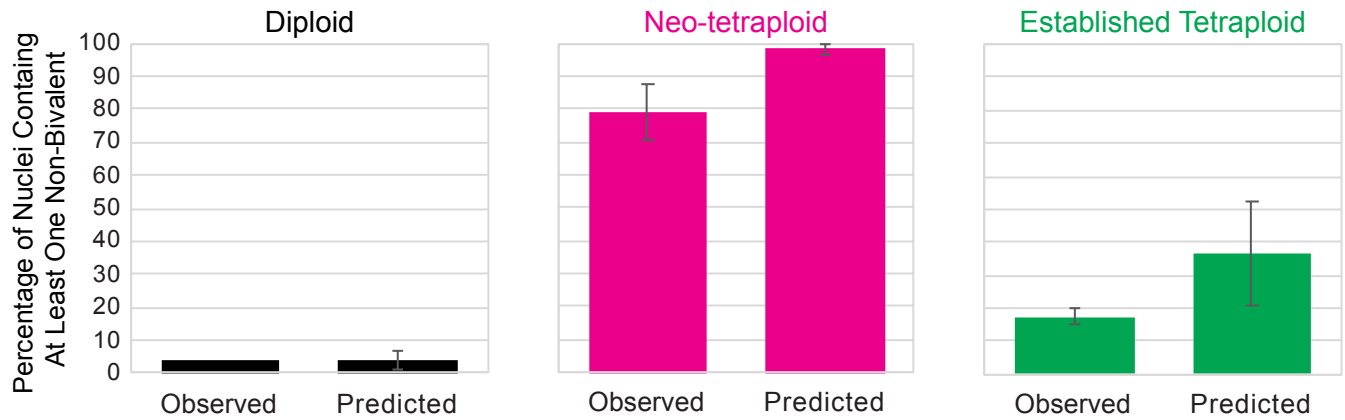


Figure S3. Observed and Predicted Metaphase I Patterns. Related to Figure 1. The observed percentage of nuclei with at least one non-bivalent structure (univalent or multivalent) and the percentage predicted from observed pachytene HEI10 foci patterns for diploid, neo-tetraploid and established tetraploid. Error bars show standard error of the mean. N = 1, 2, and 4 plants for observed diploid, neo-tetraploid and established tetraploid values. N = 4 plants for predicted values for diploid, neo-tetraploid and established tetraploid. No statistically significant difference between observed and predicted values was obtained for diploid ($p = 0.67$), neo-tetraploid ($p = 0.19$), nor established tetraploid ($p = 0.17$); Wilcoxon rank sum test.

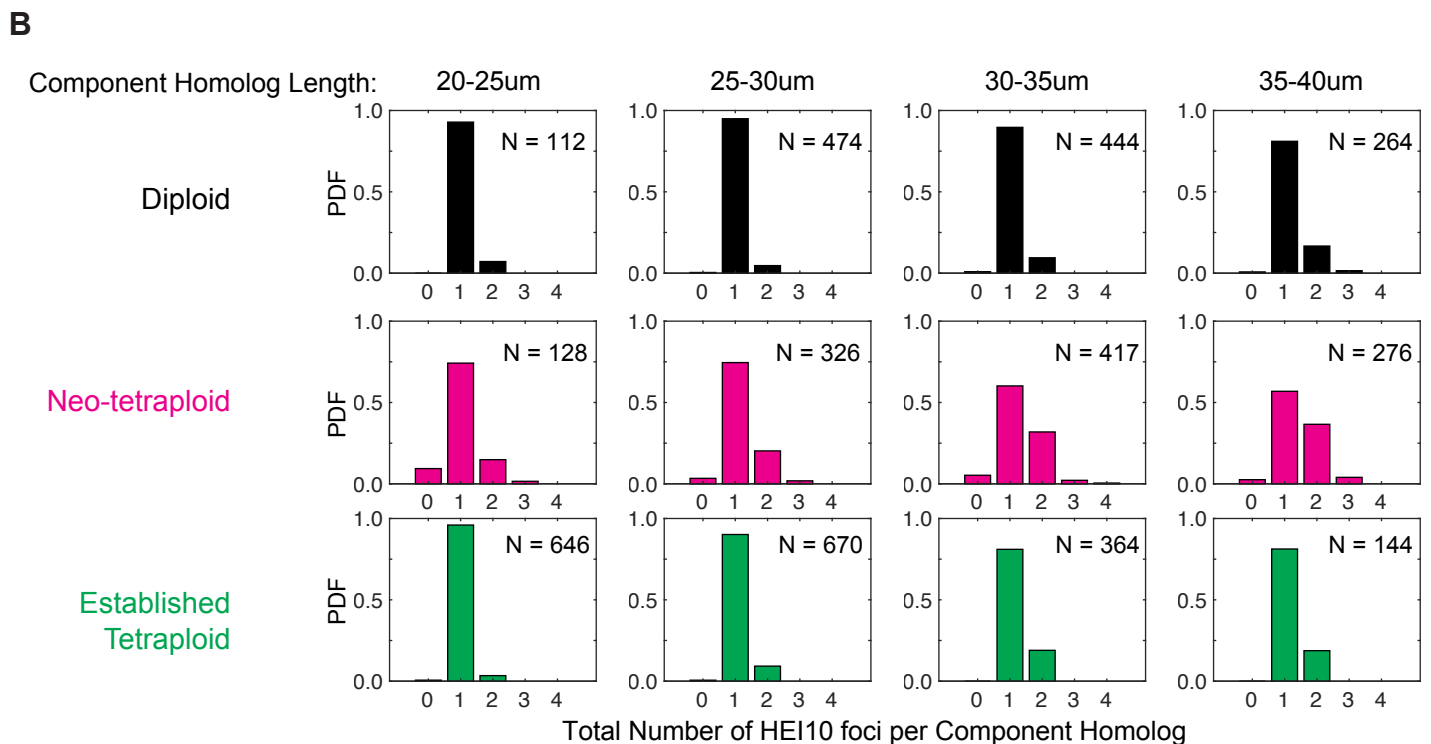
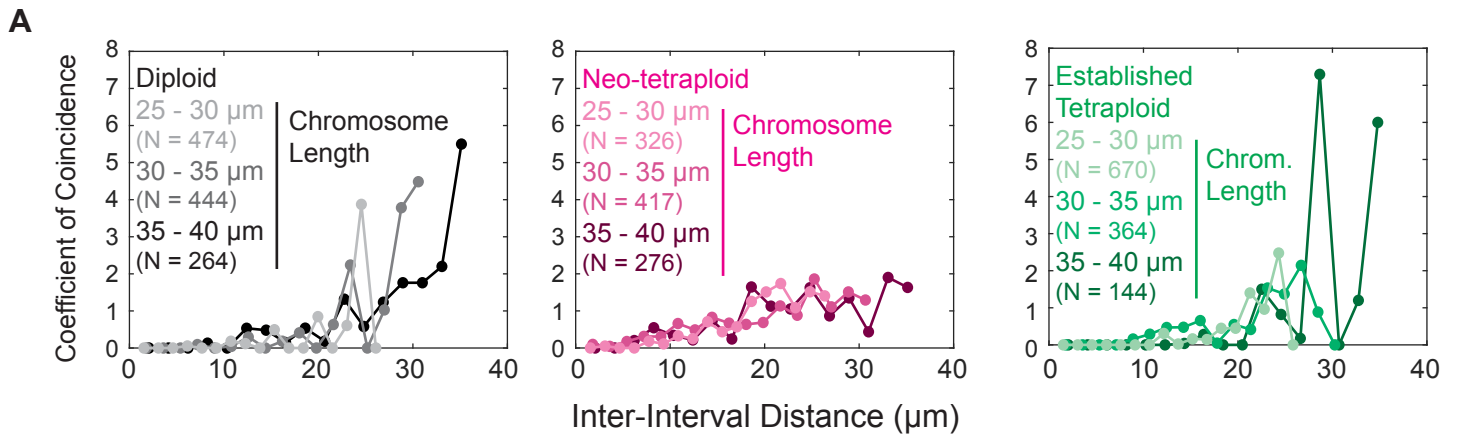


Figure S4. Component Homolog Length and Crossover Parameters. Related to Figure 4.

A. Coefficient of coincidence analysis of diploid, neo-tetraploid and established tetraploid component homologs of three different ranges of component homolog length.

B. The frequency of crossovers (HEI10 foci) on diploid, neo-tetraploid and established tetraploid component homologs of four different length bins.

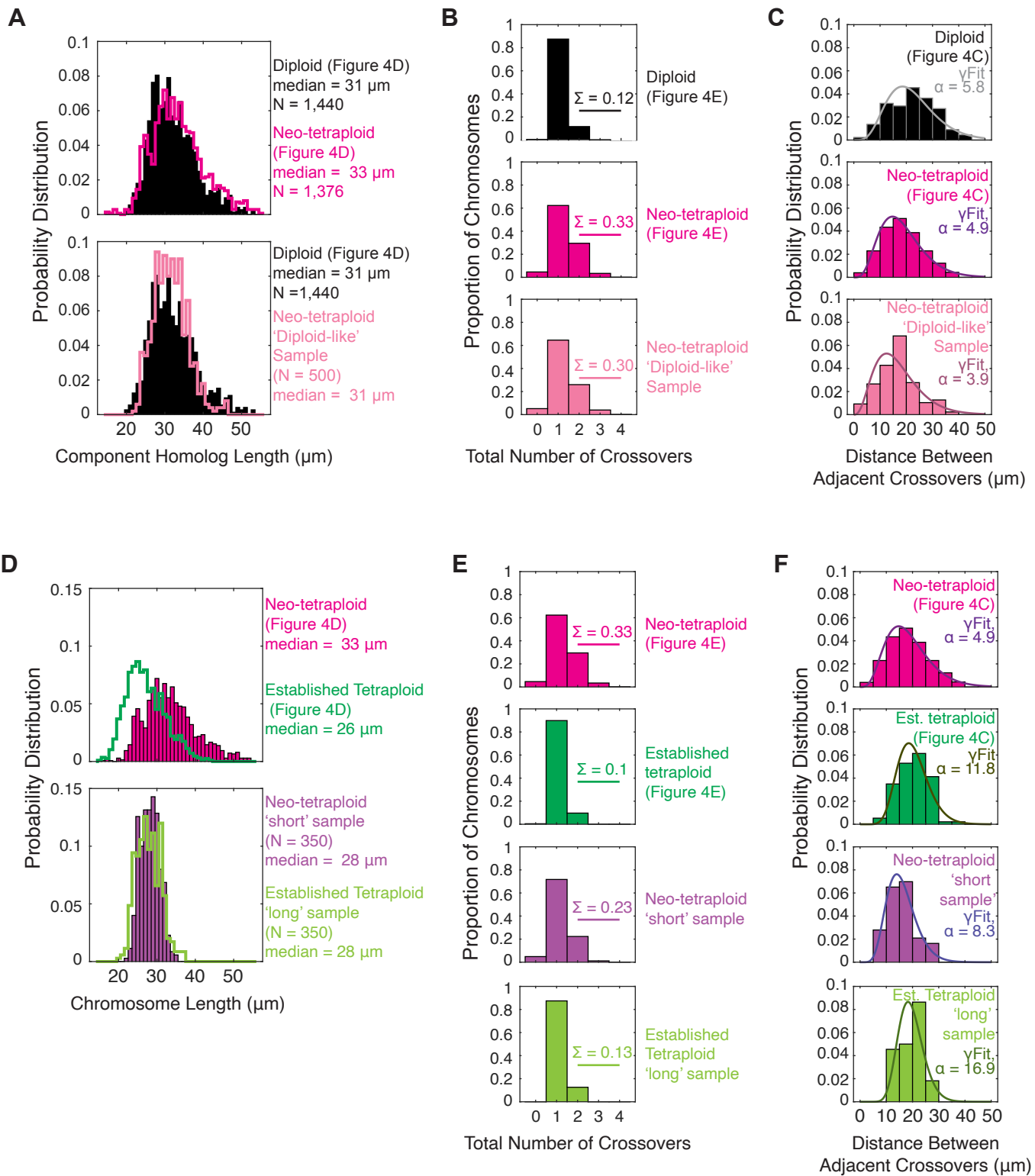


Figure S5. The effect of changes in chromosome length on crossover counts. Related to Figure 4.

A, Although neo-tetraploids have, on average, longer chromosomes than diploids, the two distributions overlap significantly allowing a sub-sample of 500 neo-tetraploid component homologs with diploid-like lengths to be obtained using the custom MATLAB function `generateMatchingLengthDistribution` of program `EvolvingStablePolyploidy v1.0.0`. The crossover patterns of this diploid-like subsample of neo-tetraploid chromosomes were analyzed. The distribution of component homolog lengths are shown. For the diploid and neo-tetraploid 'diploid-like' samples, $p = 0.33$, Wilcoxon rank sum test.

B, distribution of numbers of crossovers per component homolog with the sum of those with two or more crossovers indicated. For the diploid and neo-tetraploid 'diploid-like' samples, $p = 7 \times 10^{-13}$; Wilcoxon rank sum test.

C, distribution of distances between adjacent crossovers with shape parameter (α) of best-fit gamma distribution (`yFit`). For the diploid and neo-tetraploid 'diploid-like' samples, $p = 6 \times 10^{-10}$; Wilcoxon rank sum test.

D, a sample of 350 neo-tetraploid and 350 established tetraploid component homologs of comparable length were generated using the custom MATLAB function `generateMatchingLengthDistribution` (neo-tetraploid 'short' sample and established tetraploid 'long' sample respectively; $p = 0.12$; Wilcoxon rank sum test.

E, distribution of numbers of crossovers per component homolog with the sum of those with two or more crossovers indicated. For the neo-tetraploid 'short' sample and established tetraploid 'long' sample, $p = 0.02$; Wilcoxon rank sum test.

F, distribution of distances between adjacent crossovers with shape parameter (α) of best-fit gamma distribution (`yFit`). For the neo-tetraploid 'short' sample and established tetraploid 'long' sample, $p = 1 \times 10^{-4}$; Wilcoxon rank sum test.

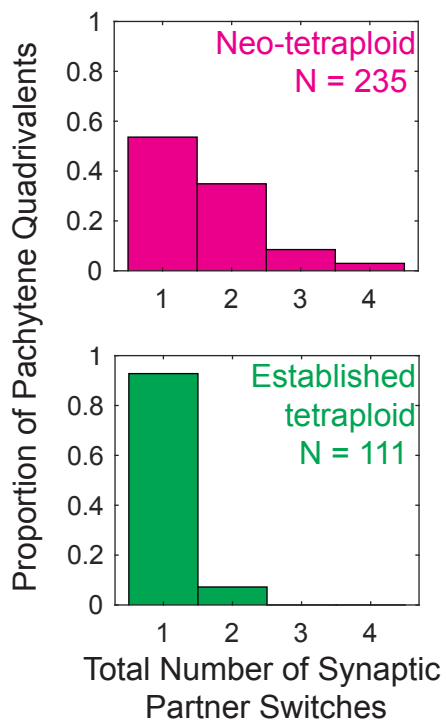


Figure S6. Distribution of total number of synaptic partner switches. Related to Figure 6. Distributions of total number of synaptic partner switches in pachytene quadrivalents.